Transformations between Polyiodide Structures in a Nylon 6 Matrix

N. S. Murthy* and Y. P. Khanna

Research and Technology, Allied-Signal Inc., P.O. Box 1021, Morristown, New Jersey 07962

Received November 30, 1992. Revised Manuscript Received February 25, 1993

Nylon 6 (N6) can incorporate up to 1.4 times its weight of iodine, and this is the highest reported for any polymer–iodine complex. Structures of these complexes are investigated by X-ray diffraction. Iodine exists in the N6 matrix as iodide ions between hydrogen bonded sheets. The heavily iodinated N6 (1.25 mol of iodine/chemical repeat of N6) shows an equatorial period of 23 Å which we attribute to the presence of I_5^- arrays perpendicular to the chain axis. The complex rapidly loses iodine during initial aging and becomes fairly stable once a concentration level of ca. 0.75 mol of iodine is reached. During this initial aging, the I_5^- arrays transform into I_3^- species but maintain their orientation and thus result in a structure with an equatorial 15.6 Å repeat. As the concentration of the iodide ions is further reduced by continued aging (0.25 moles), the I_5^- columns are established parallel to the chain axis, resulting in a structure with an equatorial repeat of 8 Å. Thermal data show that the transition from $I_3^-(\perp)$ to $I_5^-(\parallel)$ is the result of "melting" and "recrystallization" of the iodide ion arrays. The γ form of N6 is obtained as the iodide ions are removed from the 8-Å structure. A lattice match between the $I_5^-(\parallel)$ ions and the chain-axis structure of N6 in the final stage of the complex is thought to be responsible for the formation of the γ crystalline form of N6 from the iodinated complex.

Introduction

Iodine, because of its high electronegativity, is extensively used as an active cathode material in dry lithium galvanic cells.[1] But, it is difficult to mold iodine, and iodine has poor electrical conductivity. Therefore, most common lithium iodide batteries use iodine supported by polymers such as poly(2-vinylpyridine).[2] The conductivity of these polymer–iodine adducts is higher than that of pure iodine, and thus the internal resistance of the galvanic cell is lowered. The conductivity of the polymer–iodine complex depends on the concentration of iodine. The structure of iodine ions in polymer–iodine complexes has been investigated in considerable detail.[3-15] Iodine in polymers exists most frequently as I_3^- ions, but depending on the concentration of iodine, other forms of iodide ions have also been observed.[6] The transformation between the various structures is important in understanding the voltage/energy characteristics of the galvanic cells.

In this report, we discuss the structure of iodide ions and the transformation between different iodide ion species in a nylon 6 (N6) matrix. The motivation is that N6 stores the largest amount of iodine than any other polymer and it is a good solid-state electrolyte. Furthermore, the high crystalline order found in N6–iodine (N6–I) complexes has not been observed thus far in other nylon–iodine complexes.[10-15] In our earlier publications, we reported two structures with 15.6- and 8-Å equatorial repeats.[10,13] Resonance Raman spectroscopic measurements of Burzynski et al. showed that the 15.6-Å structure is associated with I_3^- ions perpendicular to the chain axis, and the 8-Å structure is associated with I_5^- columns parallel to the chain axis.[11] We proposed that the presence of I_3^- and I_5^- arrays in every other iodine layer between the hydrogen bonded sheets in the complex can account for the 15.6-Å repeat. The I_5^- columns between the hydrogen-bonded sheets was proposed to explain the 8-Å spacing.[13] While pursuing the unique structural features of N6–I complexes, we have found a new structure in freshly prepared complexes. We present here this new 23-Å structure, revise the structural models proposed earlier, and discuss the thermal analysis results pertaining to the structural transitions in these complexes.

Materials and Methods

N6 film from Allied-Signal (Capran 77A, 25 μm thick, M_w = 38 000, $M_w/M_n \sim 2$) was the starting material. As-received unoriented films as well as uniaxially oriented film, obtained by stretching the film by ca. 3×, were used. The films were iodinated by immersing the film in an aqueous solution of 1.23 N KI and 1.23 N I_2 at room temperature for 5 min to 1 h. The complexation was essentially complete in the first 5 min in these thin films. The films were then rinsed with water for ~2 min to remove excess iodine from the surface of the films.

The iodinated film in this first stage of iodination is air-sensitive and rapidly loses iodine, a point that went unnoticed in our earlier work. Therefore, the state of iodination in these fresh films was

* To whom correspondence should be addressed.

(1) Yamamoto, T.; Kuroda, S.-I. *J. Electroanal. Chem.* **1983**, *158*, 1.
(2) Schneider, A. A.; Harney, D. E.; Harney, M. J. *J. Power Sources* **1980**, *5*, 15.
(3) Hinrichs, W.; Buttner, G.; Steifa, M.; Betzel, C.; Zabel, V.; Pfannemiuler, B.; Saenger, W. *Science* **1987**, *238*, 205.
(4) Oishi, Y.; Yamamoto, H.; Miyasaka, K. *Polym. J.* **1987**, *19*, 1261.
(5) Matsubara, I.; Magill, J. H. *Polymer* **1966**, *7*, 199.
(6) *Extended Linear Chain Compounds*; Miller, J., Ed.; Plenum: New York, 1982.
(7) Baughman, R. H.; Hsu, S. L.; Pez, G. P.; Signorelli, A. J. *J. Chem. Phys.* **1978**, *68*, 5405.
(8) Hsu, S. L.; Signorelli, A. J.; Pez, G. P.; Baughman, R. H. *J. Chem. Phys.* **1978**, *69*, 106.
(9) Murthy, N. S.; Miller, G. G.; Baughman, R. H.; *J. Chem. Phys.* **1988**, *89*, 2523.
(10) Murthy, N. S.; Szollosi, A. B.; Sibilia, J. P.; Krimm, S. *J. Polym. Sci., Polym. Phys.* **1985**, *23*, 2369.
(11) Burzynski, R.; Prasad, P. N.; Murthy, N. S. *J. Polym. Sci., Polym. Phys. Ed.* **1986**, *24*, 133.
(12) Chuah, H. H.; Porter, R. S. *Polymer* **1986**, *27*, 241.
(13) Murthy, N. S. *Macromolecules* **1987**, *20*, 309.
(14) Murthy, N. S.; Hatfield, G. R.; Glans, J. H. *Macromolecules* **1990**, *23*, 1342.
(15) Kawaguchi, A. *Polymer* **1992**, *33*, 3981.

0897-4756/93/2805-0672$04.00/0

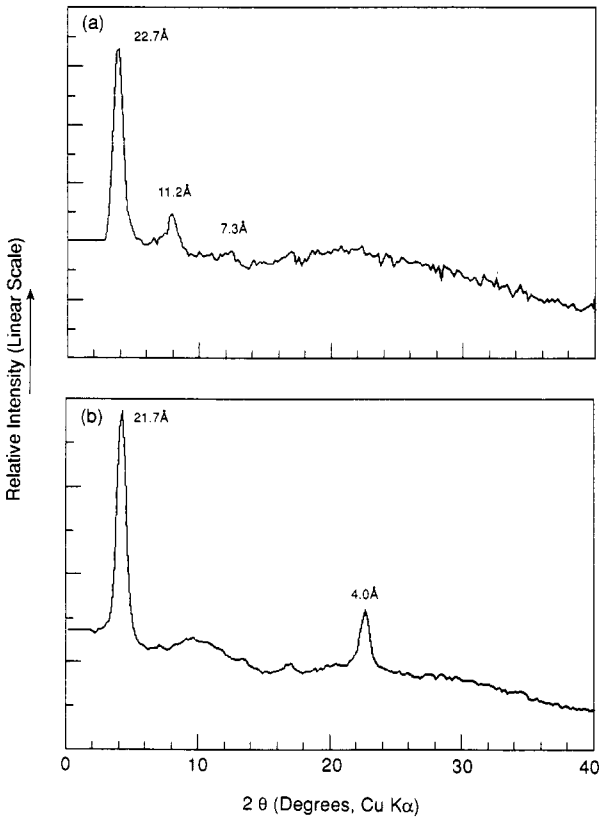

Figure 1. Wide-angle X-ray diffraction scans obtained from freshly prepared N6–I complexes showing low-angle reflections which we attribute to a new 23-Å structure. (a) Three orders of the 23-Å repeat; (b) an additional 4-Å spacing. The differences in the *d* spacing of the low-angle peak in the two scans reflect the variability in the structure of the complex due to sample preparation.

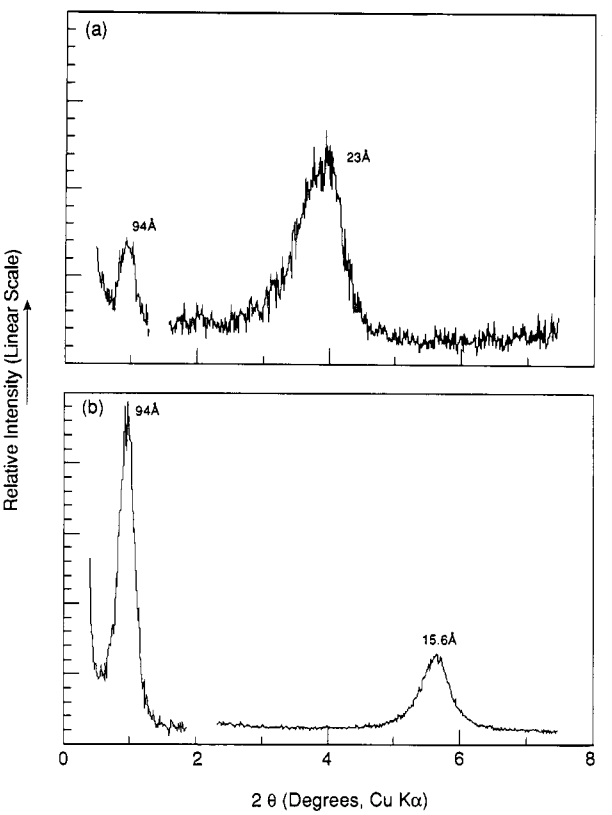

Figure 2. Composites of meridional small-angle (left part of the scans) and equatorial medium-angle scans (right part of the scans) showing the lamellar repeat and the reflections due to the N6–I complex with in the lamellae. The 23-Å reflection is observed in freshly prepared samples (a) and the 15.6-Å reflection is observed in aged samples (b).

preserved during measurement by sealing them in X-ray quartz capillaries.

The film at the second stage of iodination was obtained by further washing the film for ~15 min. These samples were stable for several days under ambient conditions and hence were analyzed without sealing in any capillary.

To obtain the film in the third and the final stage of complexation, the film was washed in an aqueous solution of sodium thiosulfate, $Na_2S_2O_3$. The extent of leaching was controlled by varying the duration for which the film was immersed in $Na_2S_2O_3$, and the rate of leaching was controlled by further diluting the stock (1.23 M) solution of $Na_2S_2O_3$. The complex also undergoes iodine depletion as it ages under ambient conditions. Aging was accelerated by heating the film at 40–100 °C under dynamic vacuum.

X-ray diffraction (XRD) data were acquired in several different ways. A two-circle Huber diffractometer was used in transmission geometry for films sealed in a capillary and for uniaxially oriented films. The intensity data either were step scanned using a scintillation detector or were obtained from the image on a Siemens area detector. XRD data from non-air-sensitive, unoriented films were obtained in parafocus geometry on a Philips diffractometer. Small- and medium-angle XRD scans were obtained on a Franks' camera using a 1-D position-sensitive proportional counter.

Differential scanning calorimetry (DSC) data were obtained on a du Pont 9900 instrument using ca. 10 mg of samples and a scanning rate of 10 °C/min. Thermal gravimetric analysis (TGA) data were obtained on a Perkin-Elmer TGS-2 unit using ca. 4 mg of samples and a heating rate of 10 °C/min.

Results

Wide-angle XRD scans obtained from two unoriented N6 films corresponding to different levels of initial rinsing are shown in Figure 1. Figure 1a shows up to three orders of a 23-Å spacing; the higher orders are not exact multiples of the 23-Å repeat probably because of the large errors in the *d* spacings at these low angles. These low-angle reflections were not observed in our earlier work. The repeat period corresponding to these reflections varies from 21.5 to 24.5 Å, and such changes in *d* spacings are not uncommon in polymer complexes. Figure 1b shows the low-angle peak at 21.7 Å and an additional 4-Å reflection which could be an equatorial spacing unrelated to the low-angle reflection (see Discussion). The two figures illustrate our observation that there can be a large variability in the structure of the complex associated with the low-angle reflection. This new structure is more disordered than other N6–I complexes, and variability could arise because of the sensitivity of this structure to the degree of hydration and aging. For convenience we will identify this new structure by its average 23-Å spacing.

A composite of the meridional small-angle and equatorial medium-angle XRD scans from an uniaxially oriented, freshly prepared N6–I complex is shown in Figure 2a. In addition to the equatorial 23-Å spacing seen in the unoriented heavily doped samples, this figure shows a lamellar reflection at 94 Å along the chain axis. Upon washing, the 23-Å peak shifts to 15.6 Å, while the lamellar spacing remains unchanged except for the change in intensity (Figure 2b).[13] This 15.6-Å peak was reported in our earlier publications and corresponds to a structure in which I_3^- ions are perpendicular to the chain axis. This second stage of the complex will be referred to as the 16-Å structure in the remainder of the paper.

Although the concentration of iodine in the N6–I complex can be controlled by the molarity of KI and I_2 in the solution used to prepare the samples, for historical

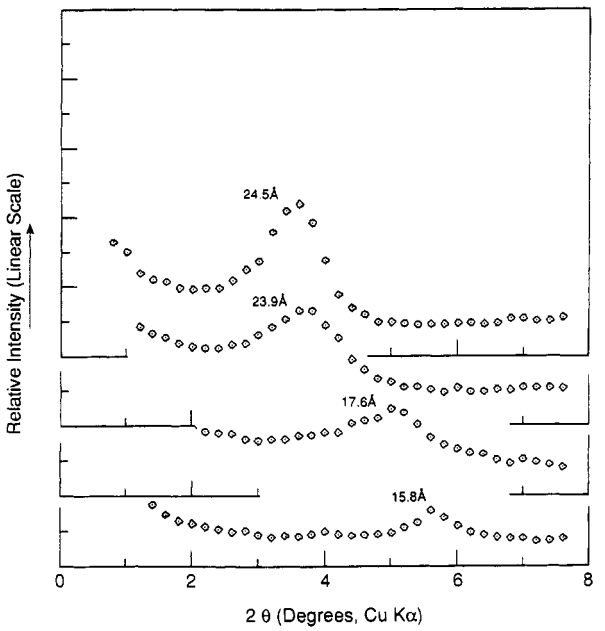

Figure 3. Small-angle X-ray scans showing the evolution of the 16-Å spacing from the 23-Å spacing in a N6–I complex. These data were obtained as the fresh complex was continuously washed in water. Data were collected at 0.015° 2θ intervals, but the intensities of 13 neighboring points are averaged and the data plotted at 0.2° 2θ intervals.

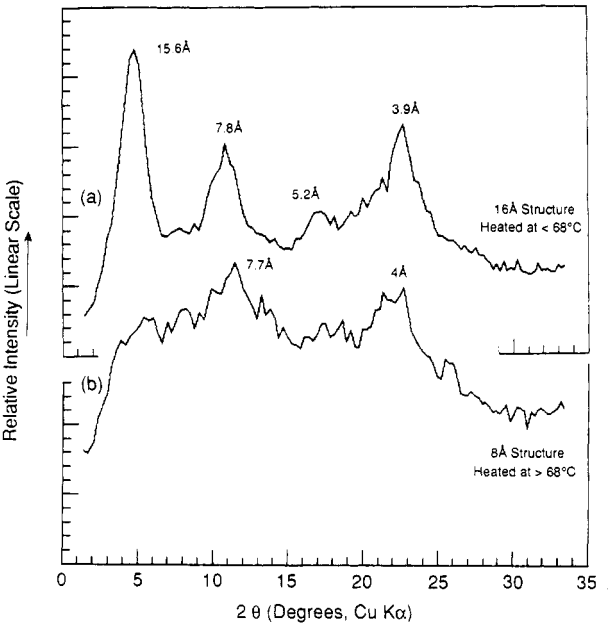

Figure 4. Wide-angle X-ray scans derived from area detector images of the N6–I complex. (a) Four orders of the structure with 15.6-Å spacing are seen in the second stage of iodination of a sample aged at $T < 68$ °C. (b) The 15.6-Å series of spacings are replaced by two orders of ~8-Å spacing in the third stage of iodination obtained by heating at ~60 °C for 100 s.

reasons we varied the iodine concentration by controlling the extent of iodine desorption. Iodine was removed from the complex by washing in water or in a dilute solution of aqueous sodium thiosulfate, or by drying. Longer durations of washing or drying, higher concentrations of $Na_2S_2O_3$ during washing, and higher temperatures during drying lead to lower iodine concentrations. Figure 3 shows the evolution of the previously published 16-Å structure from the 23-Å structure as the complex was washed in water for about 15 min. An additional peak between the 23- and 16-Å reflections, which was occasionally observed, suggests that structures with spacing between the 23 and 16 Å could also be present.

The transformation of the 16-Å structure to the final third stage of the complex, which will be referred to as the 8-Å structure, is illustrated in Figure 4 using the XRD scans from iodinated N6 films heated for 100 s at temperatures below 68 °C and above 68 °C, respectively. The 68 °C temperature was chosen because, as shown by the DSC results given below, the complex undergoes a structural phase transition at about this temperature. The 8-Å structure can also be obtained by continued washing in aqueous solution of sodium thiosulfate and by heating at 40 °C for 1 h or at 80 °C for 4 min. Further annealing (e.g., at 100 °C for a day; 100 °C chosen because of the large weight loss observed in TGA, see below) results in a highly disordered structure with a single diffraction band at 4 Å (Figure 5a). This sample can be converted into N6 containing α and γ crystalline forms by removing the iodine by washing with an aqueous solution $Na_2S_2O_3$ (Figure 5b).

The above structural transformations were investigated by TGA and DSC. The TGA of the fresh (23-Å spacing) sample is similar to the one shown in Figure 6a in that it showed changes in the rate of weight loss at ca. 75, 125, and 185 °C, and the decomposition of the complex at 280–300 °C. Since the DSC plot of the complex in the first stage of iodination (23-Å structure) was very noisy (wet sample), thermal data from the fresh sample will not be discussed. Gravimetric analysis of the complex in the

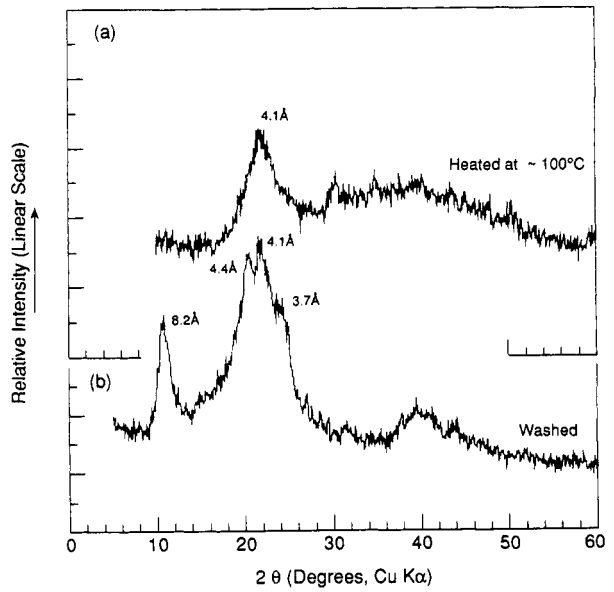

Figure 5. (a) Wide-angle XRD scans of N6–iodine complex heated at 100 °C for a day. The 4.1-Å reflection could be due to an highly disordered γ-crystalline phase, adduct or complex. (b) Mixtures of the α- and the γ-crystalline forms of N6 obtained after complete removal of iodine by washing with $Na_2S_2O_3$. The α-crystalline phase is identified by the 4.4- and 3.7-Å reflections, and the γ-crystalline phase by the 8.2- and 4.1-Å reflections. The 8.2-Å peak is a meridional reflection, and the 3.7-, 4.1-, and 4.4-Å peaks are equatorial reflections.

second stage of iodination (16-Å structure) shows major weight losses at ca. 75, 125, and 185 °C (Figure 6a). DSC scans show that these losses are accompanied by a series of thermal transitions (Figure 6b). Typically, we observe endotherms at 54 (narrow), 125 (broad), and 190 °C (broad), and broad exotherms at 71, 130–150, and 230 °C. The strong endotherm at 280–300 °C is due to the decomposition of the complex. When the complex is quenched from 60 °C (above the 54 °C transition), the only significant change in the DSC scan is the shift of the

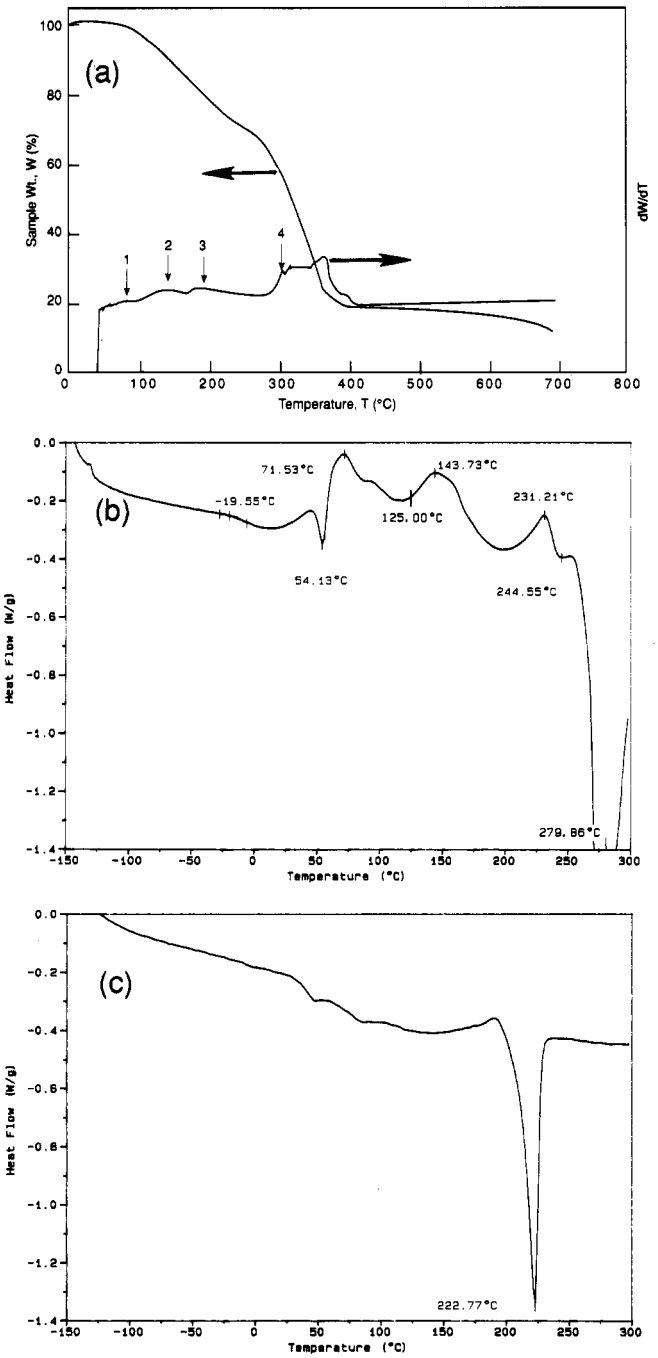

Figure 6. (a) Thermal gravimetric data showing the four frequently observed, major transitions (numbers 1–4) in the N6–I complex. (b) Differential scanning calorimetric scans showing the temperatures of the various transitions. (c) A DSC scan of N6 is shown for comparison. The maximum value on the y axis has been arbitrarily set to zero in the two DSC scans.

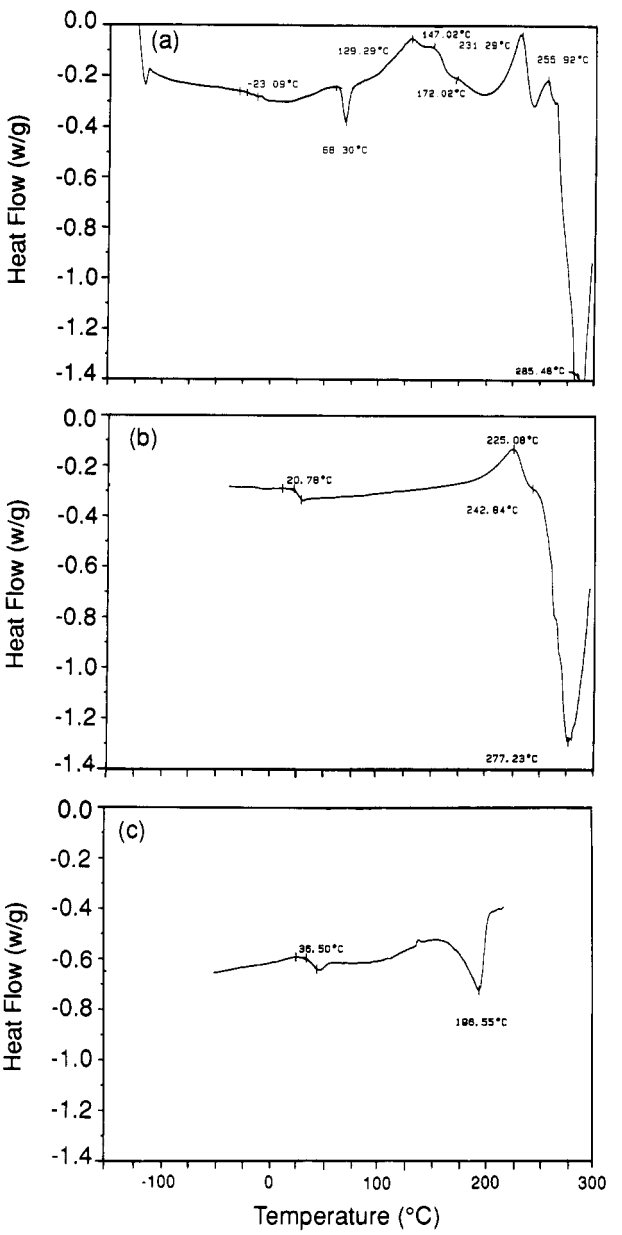

Figure 7. DSC scans of N6–I complex after various thermal treatments. (a) Quenched from 60 °C. (b) Quenched from 200 °C. (c) Aged for 1 day at 100 °C. The maximum value on the ordinate has been arbitrarily set to zero.

54 °C endotherm to 68 °C (Figure 7a). Upon quenching from 200 °C, the features below 200 °C disappear but the exotherm at 224 °C remains (Figure 7b). The DSC scan of a complex aged at 100 °C for a day (corresponding to the sample used in the XRD scan shown in Figure 5a; 100 °C selected based on the weight loss curve) shows a T_g of ≈37 °C and a broad melting at 185–195 °C (Figure 7c).

Elemental analyses show that our N6–I complexes contain the highest iodine reported for any polymer–iodine complex. The weight ratio of iodine to N6 is 1.4 compared to the maximum 0.97 reported by Yamamoto and Kuroda.[1] Typical molar compositions were $N6K_{0.18}I_{1.23}(H_2O)_{2.17}$ in fresh samples, $N6I_{0.76}K_{0.11}$ in samples rinsed with water and then dried, and $N6I_{0.3}K_{0.002}$ in partially washed samples. These three samples are representative of the complexes with the three polyiodide structures.

Discussion

The type of iodide ion arrays in the matrix and the structure of the complex is determined by the iodine concentration. XRD analyses were carried out to elucidate the different iodide ion structures in the N6 matrix. Thermal analyses were carried out to study the energetics of the transitions between the various iodide ion species.

Our structural models to interpret the XRD and thermal results are shown in Figure 8. The lateral size of a N6 chain is ca. 4.2 Å, the iodide ions within an array are ca. 3.3 Å apart, and the distance between noninteracting iodide ions is ~4.75 Å.[6,13] In the model for the heavily doped structure (Figure 8a), an I_5^- array of length 17.95 Å between two N6 chains and perpendicular to the chain axis accounts for the 23-Å repeat. The iodine concentration decreases to intermediate levels upon aging, and I_5^- transforms into

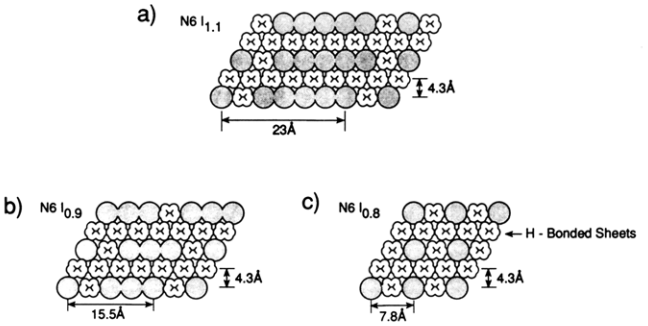

Figure 8. Proposed models for the three types of the iodide ions (open circles) in a N6 matrix. (a) $3I_5^-$ structure with 23-Å spacing. (b) $3I_3^-$ structure with 15.6-Å spacing. (c) I_5^- structure with 8-Å spacing. There is no a priori reason for the iodine sheets in adjacent layers to be in register, and therefore the iodine arrays in adjacent layers in (a) and (b) have been offset randomly along the long axis.

I_3^-. In the model for intermediate doping levels (Figure 8b), an I_3^- array of length 11.35 Å is inserted between two N6 chains and perpendicular to the chain axis to account for the observed 15.6-Å repeat. Finally, in the lightly doped structure (Figure 8c), an I_5^- column is parallel to the chain axis and is between two nylon 6 chains, thus giving rise to the 8-Å spacing. We attribute the 4-Å spacing observed in these complexes to the distance between the adjacent layers as indicated in Figure 8. It is possible that there could be structures other than the ones shown in Figure 8, as suggested for instance by the XRD scan in Figure 3; these structures are likely to be composed of mixtures of the three packing arrangements discussed above.

In our earlier publications, we reported meridional reflections due to iodide ions at 4.75 and 3.1–3.2 Å.[10,13] The 4.75-Å spacing observed in the earlier stages of the complex is the distance along the chain axis (of N6) between the I_3^- arrays or the I_5^- arrays. Since the chain-axis repeat of the complex is 15.6 Å, there can be three I_5^- or three I_3^- arrays for every crystallographic repeat of N6 in the initial stages of the complex (Figure 9a). The 3.1–3.2-Å spacing observed in the later stages of the complex is the distance between the iodide ions within an iodide ion column. On the basis of the Raman spectroscopic evidence for the orientation of the I_5^- ions parallel to the chains axis (of N6),[11] we deduce that there can be five iodide ions for each crystallographic repeat in the final stages of the complex (Figure 9b). We can thus identify the three distinct iodide ion structures in the heavily, intermediate, and lightly doped structures as $3I_5^-$, $3I_3^-$, and I_5^- species, respectively.

For each pair of CONH groups we thus have 15, 9, and 5 iodine atoms in the $3I_5^-$, $3I_3^-$, and I_5^-, structures, respectively. These correspond to 7.5, 4.5, and 2.5 mol of iodine/chemical repeat of N6, respectively. Wet chemical analysis shows that iodine concentration decreases from 1.25 mol/chemical repeat of N6 in the $3I_5^-$ structure, to 0.75 in the $3I_3^-$ structure, and finally to 0.25 in the I_5^- structure. Thus, there is a discrepancy between the calculated and the observed values. If we assume, on the basis of SAXS data,[13] that there is ca. 6 times more iodine in the crystalline regions than in the amorphous regions, there will be 3.8, 2.3, and 1.3 mol of iodine/N6 repeat in the $3I_5^-$, $3I_3^-$, and I_5^- structures, respectively. To obtain the observed values of 1.23, 0.76, and 0.3 mol of iodine/N6 repeat in these three complexes, we have to further assume that each iodide column is shared by 3–4 chains. The models proposed in Figure 8 are consistent with these arguments.

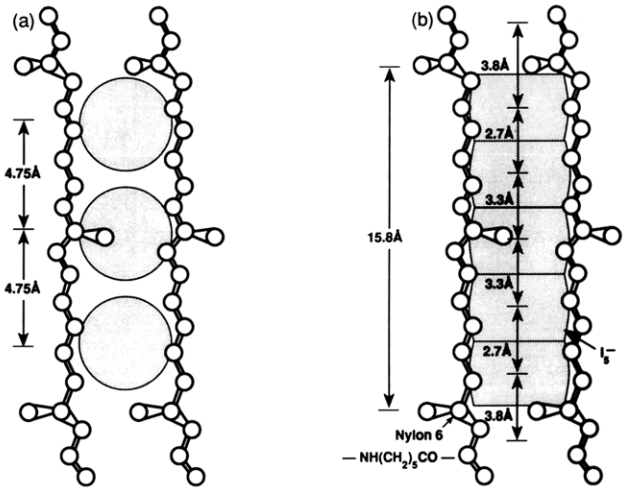

Figure 9. Chain-axis structures for the two orientation of the iodide ion species. (a) Iodide ion arrays perpendicular to the chain axis in the N6–$3I_5^-$ and N6–$3I_3^-$ complexes. (b) Iodide ion arrays parallel to the chain-axis in the N6–I_5^- complex.

TGA shows that there are at least three distinct regimes of iodine depletion: 75, 125, and 190 °C (Figure 6a). Iodine loss begins at 75 °C, accelerates at 125 °C, and slows down at 190 °C, and the complex decomposes at ca. 290 °C. The DSC scan in Figure 6b suggests that the first structural transition at 54 °C is endothermic. At about the same temperature, the XRD data shows that the 16-Å spacing disappears. Our structural models (Figure 8) suggest that the disappearance of the 16-Å repeat could be a structural phase transformation during which the $I_3^-(\perp)$ arrays become $I_5^-(\parallel)$ columns. The 54 °C endotherm can therefore be regarded as due to the "melting" of the $I_3^-(\perp)$ arrays which is followed by an exothermic formation of the $I_5^-(\parallel)$ arrays at 70 °C. The diffraction pattern of the 100 °C aged sample shows no evidence for the presence of any structured iodine, and the complex yields mixture of α and γ form (Figure 5). Therefore, the endotherm at 125 °C (Figure 6b) could be attributed to the melting of the $I_5^-(\parallel)$ columns. The 190 °C endotherm is seen in all the samples irrespective of the type of iodine structure. Since the 100 °C aged sample, which does not have a significant fraction of structured iodine, shows a 190 °C endotherm (Figures 5a and 7b), the 190 °C is most likely the melting of the N6 in the presence of iodine. The simplest explanation of the lower (190 °C) melting point of the complex compared to 222 °C in the α N6 and 213 °C in the γ N6 is that iodide ions act as impurities and thus depress the melting point. The 230 °C exotherm represents the formation of an amorphous complex of molten N6 and iodine which eventually decomposes at 275–300 °C. Thus the scheme for changes during heating is as follows:

$$\underbrace{3I_5^- \xrightarrow{\text{ambient aging}} 3I_3^-}_{\text{complexed with N6}} \xrightarrow{60\,^\circ\text{C}} I_5^- \xrightarrow{125\,^\circ\text{C}} \text{N6}\,(\alpha+\gamma)\ \text{and}\ I_2 \xrightarrow{190\,^\circ\text{C}}$$

$$\text{melting of N6} \xrightarrow{230\,^\circ\text{C}} \text{melt adduct of iodine and N6} \xrightarrow{300\,^\circ\text{C}} \text{decomposition}$$

A similar scheme can be proposed for washing as well.

As mentioned earlier, iodine can be depleted from the N6–I complex either by heating or by washing with water or an aqueous solution of $Na_2S_2O_3$. But the final structures obtained by these two methods are not necessarily the same. While washing with aqueous solution of $Na_2S_2O_3$

always yields the γ-crystalline form of N6, removal of iodine by heating can yield mixture of α and γ forms (Figure 5b) or even an amorphous N6 depending on the temperature and duration of heat treatment and the initial concentration of iodine in the film.

An important observation from our SAXS data in Figure 2 as well as from our published data in ref 13 is that a reflection corresponding to the interlamellar spacing is observed at all stages of complexation. Thus, iodination does not result in any substantial disruption of the superstructure despite the dramatic changes in the structure within the lamellae. Although the iodide ion arrays might "melt" and change the structure of the complex, the crystalline structures of the complex do not melt at any stage of iodine desorption. Thus, the endotherms seen in the DSC scans (Figure 6b) refer to the "melting" of the iodide ion arrays and the exotherms are the "recrystallization" into different types of arrays.

Finally, these highly crystalline complexes have been observed only in N6 and not in other aliphatic polyamides, not even in N6,6. One explanation is that the N6 chain is able to assume conformations with chain-axis repeat as small as 15 Å, so that the polymer chains can form commensurate structures with iodine columns. This is not possible in N6,6. On the basis of our observations, we postulate that highly crystalline complexes can occur in N12 with iodine, and in other nylons if a complex can be formed with other halogens.

Acknowledgment. We thank J. J. Belles and G. Chomyn for thermal analyses, E. I. Uyehara and J. Bitay for elemental analysis, and S. Krimm for discussions.